C. R. Physique 3 (2002) 15–27

Électromagnétisme, optique/*Electromagnetism, optics*
(Solides, fluides : propriétés électroniques et optiques/*Solids, fluids: electronic and optical properties*)

DOSSIER

MICROCAVITÉS ET CRISTAUX PHOTONIQUES
MICROCAVITIES AND PHOTONIC CRYSTALS

Strong coupling regime in semiconductor microcavities

Romuald Houdré [a], Ross P. Stanley [a], Ursula Oesterle [a], Claude Weisbuch [b]

[a] Institut de micro- et optoélectronique, École polytechnique fédérale de Lausanne, CH 1015, Lausanne, EPFL, Switzerland

[b] Laboratoire de physique de la matière condensée, École polytechnique, 91128 Palaiseau, France

Received and accepted 23 November 2001

Note presented by Guy Laval.

Abstract We introduce to the physics of semiconductor microcavities in the strong coupling regime, also known as cavity-polariton. We discuss the optical response, cavity-polariton dispersion curve, inhomogeneous broadening due to disorder effect and homogeneous broadening due to acoustic phonon scattering. We present novel effects on high quality samples on elastic scattering and parametric oscillation effects in the non-linear response under resonant excitation. To cite this article: R. Houdré et al., C. R. Physique 3 (2002) 15–27. © 2002 Académie des sciences/Éditions scientifiques et médicales Elsevier SAS

semiconductor / exciton / polariton / quantum well / quantum optics / strong coupling

Le régime de couplage fort dans des microcavités de semiconducteur

Résumé Après une introduction à la physique des microcavités optiques semiconductrices dans le régime de couplage fort, également dénommées polariton de cavité, nous discutons la réponse optique, la courbe de dispersion de polariton de cavité, les effets d'élargissement inhomogène par le désordre et d'élargissement homogène par les phonons acoustiques. Finalement, nous présentons des effets nouveaux obtenus sur des échantillons de haute qualité sur la diffusion élastique et des effets d'oscillation paramétrique dans la réponse non-linéaire sous excitation résonnante. Pour citer cet article : R. Houdré et al., C. R. Physique 3 (2002) 15–27. © 2002 Académie des sciences/Éditions scientifiques et médicales Elsevier SAS

semiconducteur / exciton / polariton / puits quantique / optique quantique / couplage fort

1. Introduction

Since the early studies by K.H. Drexhage [1], P. Wittke [2], W. Lukosz [3] and D. Kleppner [4], low-dimensional photonic systems have been studied in many different fields, from atomic physics [5,6] to semiconductors [7,8], both from a fundamental point of view and for applications. Formally, an optical

transition consists in the promotion of a state:

$$|\text{initial electronic state}\rangle\,|n \text{ photons}\rangle \quad \text{toward a state:} \quad |\text{final electronic state}\rangle\,|m \neq n \text{ photons}\rangle$$

However, it is often neglected that the optical properties of an electronic state (absorption, spontaneous or stimulated emission), are not *intrinsic* to the state but also depend on the electromagnetic field the state is coupled to. As the electromagnetic field is usually the vacuum field of the free space, only the electronic state contributes significantly to structures in the spectral density of final states. The density of final states for the electromagnetic field forms an isotropic continuum responsible for the irreversible nature of the transition, and of its contribution there only remains a general relation between spontaneous and stimulated emission: the Einstein relations. In 1946 E.M. Purcell [9] noticed that if one modifies the surrounding electromagnetic field, with for example a cavity, it should be possible to change the rate of an electromagnetic transition. This comment is the cornerstone of the present interest for microcavities.

According to the level of structure induced in the electromagnetic field by the cavity, two different regimes of the light–matter interaction can be observed, the weak and the strong coupling regime. The first one leads to effects such as modifications of the radiative emission rate and pattern and its applications to high brightness microcavity light emitting diodes. The second one occurs when the quality factor of the cavity is large enough so that the structures induced in the photon density of states can be regarded as *discrete* photon modes, in other words when the interaction energy is larger than the spectral linewidth of the uncoupled eigenstates. At resonance the electronic state is now coupled to a single photon mode, the Fabry–Pérot mode of the cavity, and the coupling to the remaining non-resonant modes can be neglected in a first approximation. The eigenstates of the system are then the coherent superposition of the two uncoupled eigenstates, separated by the Rabi energy (Ω):

$$|+\rangle = C_{11}|e\rangle_{\text{at}}|0\rangle_{\text{phot}} + C_{12}|g\rangle_{\text{at}}|1\rangle_{\text{phot}}, \qquad |-\rangle = C_{21}|e\rangle_{\text{at}}|0\rangle_{\text{phot}} - C_{22}|g\rangle_{\text{at}}|1\rangle_{\text{phot}}$$

where C_{ij} are the mixing coefficients ($C_{ij} = 1/\sqrt{2}$ at resonance). Like in an ordinary coupled oscillator system the eigenstates energy vs. detuning δ ($\delta = E_{\text{phot}} - E_{\text{at}}$) shows an *anticrossing* behavior near resonance. The time evolution can no longer be described by the Fermi's golden rule and Rabi oscillations between excited states of the electronic or electromagnetic fields can occur *provided the system could be initially prepared in an uncoupled eigenstate* at time origin. Most of the physical properties such as linewidth etc. of the coupled eigenstates are the average value of the uncoupled ones pondered by the $|C_{ij}|^2$.

This effect called vacuum field Rabi splitting is well known in atomic physics [10] but is more complex in semiconductors: optical transitions form a continuum and the strong coupling regime cannot be obtained with such excitations because the dephasing time of electron–hole pairs is much shorter than the Rabi frequency. Nevertheless there are in solids atom-like excitation: excitons. Excitons represent the Coulomb-correlated electron–hole pair, which is the lowest excited electronic state of the crystal [11,12]. They can be seen as an electron–hole pair entangled in a hydrogen-like relative motion, the whole pair having a translational motion throughout the entire crystal. This delocalised state leads to an oscillator strength proportional to the crystal volume (bulk) or surface (quantum well, QW). As such the exciton has the same translational symmetry as the crystal, 3D for bulk material and 2D for QW and the wavevector remains a good quantum number. An exciton with a well defined in plane momentum, $k_{//}$, can only couple to the photon mode of the same momentum. This selection rule explains why although these states form a continuum the atomic physics picture is still valid. In analogy with the bulk case the set of the coupled eigenstates vs. $k_{//}$ holds the name cavity-polariton (CP). It should be noted that this strong coupling regime occurs in the case of a bulk material or a quantum well exciton in a planar cavity because both continuums have the same dimensionality and therefore a one to one correspondence between each state is possible. The coupled eigenstates are then true eigenstates of the crystal + field system and have an infinite lifetime in the ideal case. Luminescence can only occurs through an *extrinsic* scattering or dephasing mechanism (surface,

Table 1. Exciton–photon interactions

Bulk	Exciton 3D	Strong coupling
	Photon 3D	Exciton–polariton
	$\vec{k}_{3D}$ selection rule	Extrinsic radiative process
Quantum well	Exciton 2D	Weak coupling
	Photon 3D	Intrinsic radiative process
	$\vec{k}_{\perp}$ continuum	
Planar cavity	Exciton 2D	Strong coupling
	Photon 2D	Cavity–polariton
	$\vec{k}_{//}$ selection rule	Extrinsic radiative process

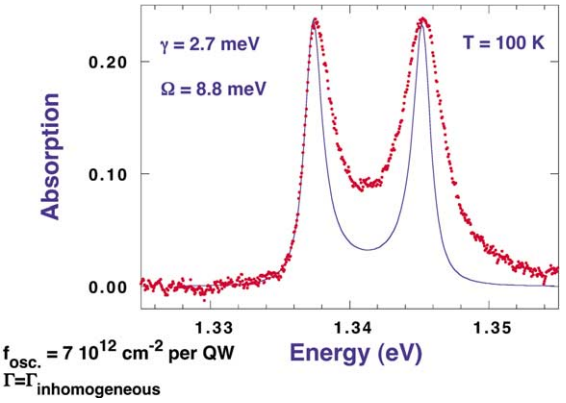

Figure 1. Vacuum field Rabi splitting observed in absorption in a $3\lambda/2$ cavity, with 6 (In, Ga)As quantum wells (from R. Houdré et al., Phys. Rev. B 49 (1994) 16761).

etc.). The case of a 2D exciton is fundamentally different because the excitonic state, being coupled to a $k_{\perp}$ continuum of photons, acquires an *intrinsic* radiative lifetime (Table 1).

Strong coupling between excitons and photons was first observed in reflectivity at low temperature by C. Weisbuch [13] and then at room temperature [14] (Fig. 1). Several models can be developed, both in linear dispersion and quantum electrodynamics theory [14–19]. As long as *classical* observables are considered these models are strictly equivalent and describe the anticrossing behavior near resonance between two coupled oscillators:

$$\Omega \propto \sqrt{\frac{f_{\text{osc.}} N_{\text{QW}}}{L_{\text{cavity}}}}$$

where $f_{\text{osc.}}$ is the oscillator strength, N_{QW} the number of quantum wells in the cavity and L_{cavity} the cavity length.

The shape of the dispersion curve of the cavity-polariton is not essential to the optical response because a single and well defined (by the geometry of the experiment) pair of coupled states is probed. However this is not the case for photoluminescence experiments because during the thermalization process a whole set of states with different $k_{//}$ are involved. Angle resolved experiments allow the direct measurements of different $k_{//}$ states and hence reveal the cavity-polariton dispersion curves [20] (Fig. 2).

Dispersion has proved to be essential to understand photoluminescence spectra and dynamics. For a while it was hoped that strong coupling would lead to a new fast and efficient recombination channel in

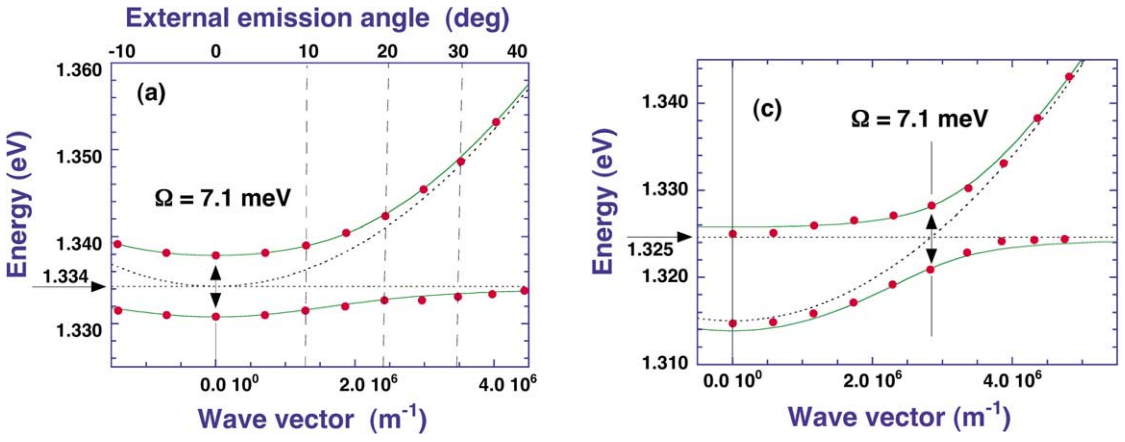

(a) (b)

Figure 2. Cavity–polariton dispersion curves: (a) zero detuning; (b) negative detuning (from R. Houdré et al., Phys. Rev. Lett. 73 (1994) 2043.

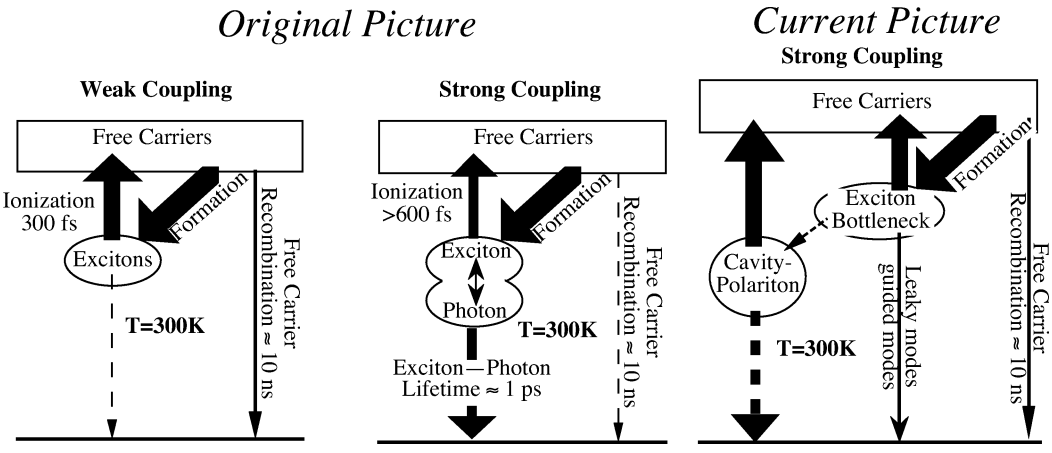

Figure 3. Thermalization and bottleneck effect in the photoluminescence of cavity-polariton, original and current picture.

semiconductors at room temperature: whereas in weak coupling excitons are readily ionized after formation before recombining, the strongly coupled exciton can decay radiatively very fast before re-ionizing with a lifetime of the order of twice the photon lifetime in the empty cavity (Fig. 3). However the first hint that this picture was not correct occurs when it was noticed that even at very low temperature, continuous wave spectra are still thermalized [21]. It was further shown theoretically and experimentally that a relaxation bottleneck occurs; due to the peculiar shape of the CP dispersion curve there is a very slow energy relaxation towards the fast emitting CP states and population build up in states of higher momentum which decay either non radiatively or radiatively in the guided mode or the leaky modes of the DBR in the GaAs substrate [22].

2. Linear response, disorder effect

Although the bottleneck effect led to the end of most foreseen wide scale applications (e.g. high-efficiency emitters), it turned out that the physical properties of CPs are much richer and complex than originally thought. As explained above they are coupled exciton/photon excitations and in some aspect these elementary excitations behaves like cavity–photon and for others like excitons: for instance, *CPs have a photon-like dispersion curve*, at least in a very narrow region of the Brillouin zone and moreover the dispersion curve can be engineered via the detuning and the interaction energy (proportional to $\sqrt{N_{\mathrm{QW}}}$). This leads to a curvature of the polariton dispersion curve 10^4 larger than the curvature of the bare exciton. It would be tempting, but confusing to translate this in a CP effective mass 10^4 lighter than the exciton effective mass [23,24]. The difficulty arises from the fact that the polariton is a very light quasi particle but only in a very limited k-space domain, this is quickly meaningless for any physical property involving nonelastic processes. On the other hand, *CPs interact like excitons* as the photon part of the CP eigenstate does not contribute to interactions. As it will be discussed below they are sensitive like excitons to material disorder such as alloy and interface fluctuations, leading to inhomogeneous broadening effects and to phonons, leading to homogeneous broadening effects.

In the atomic physics case, most of the physical properties such as linewidth, etc., of the coupled eigenstates are the average value of the uncoupled ones pondered by the $|C_{ij}|^2$. The situation is much more complex in the semiconductor case and departs significantly from the atomic case. Difficulties arise whether properties like linewidth are determined by interaction of the uncoupled states or by the coupled system.

Disorder effect in QW leads to inhomogeneous broadening in the 1 meV range. In good CP samples disorder effects can be as low as 50 μeV, due to a disorder averaging over a much larger region of the order of the cavity mode size (10 μm) instead of the exciton mode size in QW (100 Å). A theoretical description of the effects (often incorrectly referred to as motional narrowing) was first given in one-dimension by Savona et al. [25] and then in 2D by Whittaker [24]. The whole effect can be equally understood using a linear dispersion theory (LDT) approach, both theoretically [26] (Fig. 4) and experimentally [27] with an *asymmetric* exciton line.

The simple physical picture of LDT is that in order to form a FP resonance the cavity round-trip phase shift has to be an integer multiple of 2π. Due to the form of the real part of the Lorentz oscillator refractive index, the round trip phase shift vs. photon energy becomes N-shaped, up to a point where the phase shift conditions are fulfilled three times. This gives rise to the doublet structure because the central solution, which also corresponds to a maximum of absorption, does not create a FP resonance. Extension of this method to a set of non-identical oscillators, corresponding to a pure spectral disorder (i.e. no in-plane spatial disorder but a set of oscillators of different energy) is performed in replacing ε by:

$$\varepsilon(\nu) = n(\nu)^2 = \varepsilon_\infty + \sum_i \varepsilon_i(\nu) \text{ or } \int_{-\infty}^{+\infty} \varepsilon(\nu, \nu_0) g(\nu_0)\, \mathrm{d}\nu_0$$

where $g(\nu_0)$ is the spectral density of oscillators at the frequency ν_0.

Simulations are shown in Fig. 4. The absorption spectrum exhibits two main lines and residual structures of lower optical activity at the resonance energy. The existence and the peak separation of the splitting in absorption are *independent* of the homogeneous or inhomogeneous nature of the electronic oscillator. This can easily be understood considering that no specific distinction between inhomogeneous and homogeneous lines is made in this linear dispersion model. The refractive index, n, is only a function of the integrated absorption via the Kramers Kroenig transformation (K.K.), which is linear. Fig. 4 illustrates that for large splittings the linewidth is given by the *homogeneous* linewidth. As can be seen when increasing the interaction energy, the linewidth $\Delta_\pm$ of the Rabi split lines decreases from $(\sigma + \gamma_{\mathrm{photon}})/2$ to $(\gamma + \gamma_{\mathrm{photon}})/2$. This can be understood from a property of the plasma dispersion function (i.e. the

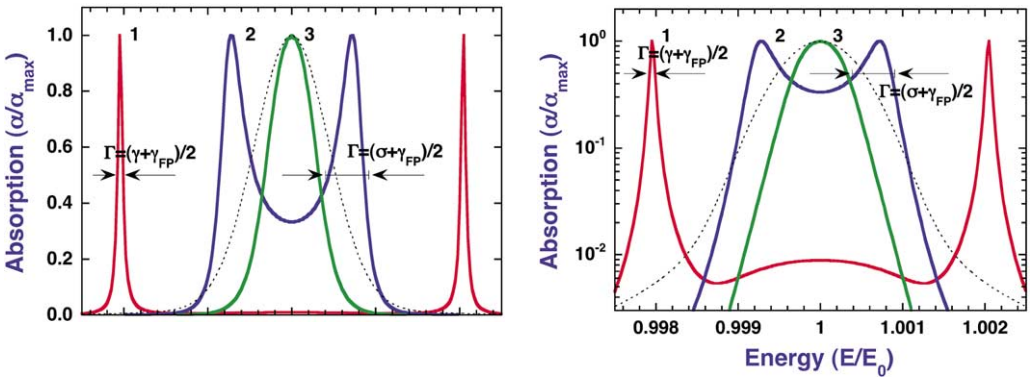

(a) (b)

Figure 4. Absorption spectrum of vacuum field Rabi splitting (Ω) for an inhomogeneously broadened system. Dashed line: absorption spectrum of the uncoupled electronic oscillator (plasma dispersion function), $\sigma = \gamma_{\text{inhomogeneous}}$, $\gamma = \gamma_{\text{homogeneous}}$), (1) strong interaction energy ($\Omega \gg \sigma$), (2) moderate interaction energy ($\Omega \approx \sigma$), (3) small interaction energy: weak coupling regime: (a) linear and (b) logarithmic scales. Parameters are: $\gamma_c/E_0 = 3 \cdot 10^{-5}$, $\gamma/E_0 = 1 \cdot 10^{-4}$, $\sigma/E_0 = 1 \cdot 10^{-3}$, the relative coupling strength are 50 (1), 5 (2) and 1 (3) (from R. Houdré et al., Phys. Rev. A 53 (1996) 2711).

convolution of a Gaussian and a Lorentz function) stating that the central energy region has a Gaussian shape while out in the wings ($\nu - \nu_0 \gg \sigma$) the function has a Lorentzian shape (see Fig. 4, log. scale). As the linewidth is determined by the slope of the round trip phase shift vs. energy function, this explains the linewidth reduction. Such models applied with a more realistic (or measured) asymmetric lineshape exciton line have been shown to be in perfect agreement with experimental observation and up till now it has not been possible to show quantum effects in the linear response of CPs, even if quantum models do sometimes provide easier to handle pictures.

Very similar conclusions can be drawn from a simple quantum model with spectral disorder and it can be shown [26] that to the first order in perturbation the $n+1$ quasi degenerated states (n electronic oscillator and 1 photon mode) gives $n-1$ uncoupled states at the resonant energy and only two states separated by the same Rabi as in an homogeneous case (i.e. $\sqrt{n}\Omega$) and eigenstates are a *collective* excitation of the whole set of electronic oscillators:

$$|\pm, 0\rangle = \frac{1}{\sqrt{2}}\left(|g..g\rangle|1\rangle \pm \frac{1}{\sqrt{n}}\sum_{i=1}^{n}|g..e_i..g\rangle|0\rangle\right) = \frac{1}{\sqrt{2}}\left(|g..g\rangle|1\rangle \pm \frac{1}{\sqrt{n}}C^{+}|g..g\rangle|0\rangle\right)$$

3. Linear response, acoustic phonon scattering

Because of the very peculiar shape of the CP dispersion curve, homogeneous broadening of the lower CP state can be reduced to value as low as 100 μeV. Photons at these energies do not interact strongly with acoustic phonons so it is the exciton part of the CP that determines the scattering and which have been calculated in the Born approximation taking into account the confinement of the QW exciton. The exciton broadening at $k = 0$ is given by the sum of the transition rates to all possible final states. Assuming the same electron and hole masses, one obtains for the broadening:

$$\Gamma_{\text{ex}} = \frac{\hbar|Q_{\text{cv}}|^2}{2\pi\rho u}\int_0^{\infty}\frac{E(k')^2}{(\hbar u)^2}\frac{1}{|\hbar u q_z|}\left|I_{\parallel}(k')\right|^2\left|I_{\perp}(q_z)\right|^2\frac{k'}{e^{\beta E(k')}-1}\,dk'$$

where ρ and u are the density and longitudinal sound velocity in GaAs respectively, Q_{cv} is the deformation potential and $E(k')$ is the exciton dispersion relation. Here q_z is given by energy conservation and is found from $\hbar u\sqrt{q_z^2 + k'^2} = E(k')$. The terms $I_{\parallel}(k')$ and $I_{\perp}(q_z^0)$ are the superposition integrals of the exciton envelope function with the phonon wave function in the in-plane and z directions, respectively. Both superposition integrals introduce cut-offs in wavevector space. The important cut-off for (In, Ga)As, is the one in the z direction and corresponds to $q_z \approx 3\pi/L_{qw}$. If we neglect the in-plane phonon dispersion, which is nearly flat compared to the exciton dispersion, we have $\hbar u q_z \approx E(k')$, and the cut-off in q_z becomes equivalent to a cut-off in the energy exchanged in the phonon absorption (or emission), and $|I_{\perp}(qz)| \approx \theta(E_{cut} - E)$. The cut-off energy, E_{cut}, comes from the limited overlap of phonons propagating in the z direction and the QW exciton when the phonon wavelength is much smaller than the QW width. For a QW of width, L_{qw}, $E_{cut} = \hbar u 3\pi/L_{qw}$. The temperature dependence can be seen by taking the limit of $k_b T > E_{cut}$ then Γ_{ex} reduces to: $\Gamma_{ex} \approx bT$, which gives the standard linear temperature dependence of the exciton linewidth. Substituting the standard values for the constants in GaAs and taking $E_{cut} = 3$ meV, then $b \approx 5$ μeV/T for the full width half maximum.

Lower polariton branch (LPB) scattering is shown schematically in Fig. 5 (lower panel). Polaritons at $k = 0$ are mainly scattered to region B. Scattering to A is reduced due to the low density of polariton states. There is no scattering to energies greater than E_{cut} (region C). For upper branch polaritons, there is the possibility of both absorption and emission of phonons (see Fig. 5 upper panel) and no inhibition effects

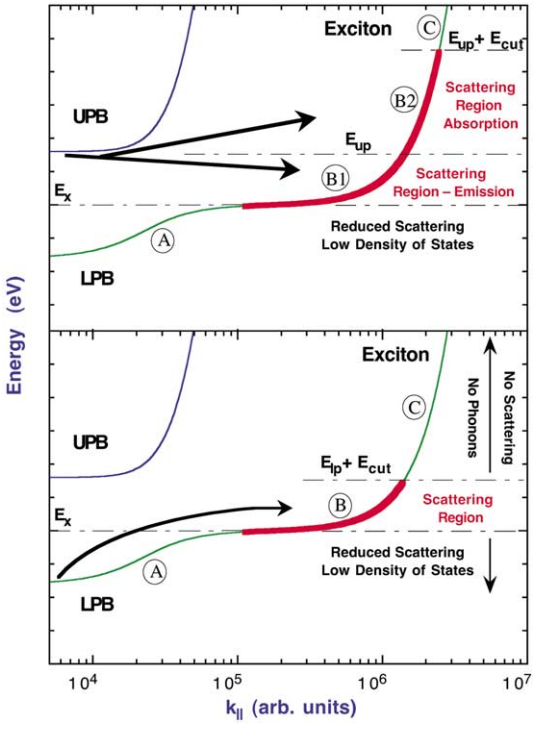

Figure 5. Dispersion curves of cavity-polaritons showing the allowed phonon scattering channels for $k = 0$. Upper panel shows absorption and emission scattering of the upper polariton branch (UPB); lower panel shows scattering for the polariton branch (LPB). Note the log scale for $k_{//}$.

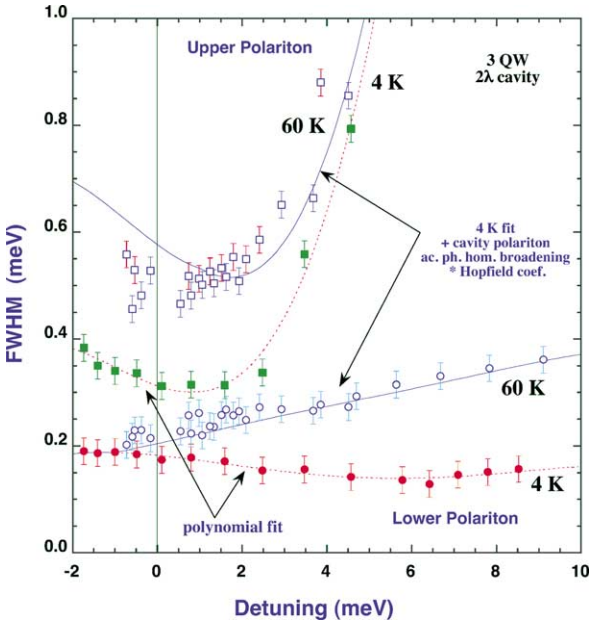

Figure 6. Linewidth of upper (squares) and lower (circles) lines derived from reflectivity spectra. Solid symbols are at 4.2 K and open symbols are for 60 K. The dashed lines are a guide to the eye for the 4.2 K data. The solid lines are the sum of the temperature dependent acoustic phonon scattering broadening calculated at 60 K plus the 4.2 K linewidth.

are expected. The cut-off energy directly translates into a detuning cut-off for which the energy separation between the LPB at $k = 0$ and the B region is larger that E_{cut}:

$$\Delta_{\text{cut}} = \frac{(\Omega/2)^2 - E_{\text{cut}}^2}{E_{\text{cut}}}$$

Δ is positive when the cavity is at a higher energy than the exciton. For $\Delta < \Delta_{\text{cut}}$, the LPB thermal broadening is given by (3) and it is therefore negligible. As the Rabi energy increases, the detuning cut-off moves from negative to positive detuning. When $E_{\text{cut}} \approx \Omega/2$, the detuning cut-off occurs near resonance.

These effects were verified experimentally. Fig. 6 shows the linewidths of both branches as a function of cavity–exciton detuning at 10 and 60 K. At 10 K the linewidth of LPB remains almost constant with a slight minima at 6 meV detuning. In contrast the UPB is larger and its linewidth increases dramatically at around 3 meV detuning due to continuum states which introduce additional absorption. On increasing the temperature, the upper polariton branch (UPB) broadens almost uniformly with detuning. The LPB shows a broadening which decreases towards negative detuning as expected.

4. Linear response, Rayleigh scattering

Mastering of disorder and phonon broadening led to new generation of CP with low In content (In, Ga)As QW and high-Q cavity samples exhibiting linewidth as narrow as 150 µeV at 4 K for the lower CP branch and with little temperature broadening up to 100 K (Fig. 7). Effects discussed below are observed on such high quality samples.

Interference and coherence effects in elastic light scattering from disordered systems are important in many domains of physics. They have been revived by the analogies that can be made with theories and experiments developed for the propagation of electrons in disordered systems, such as the weak and strong localization regimes.

In such experiments, the light re-emitted by the system consists of:

(i) a coherent, elastic part due to *static* disorder, called resonant Rayleigh scattering (RRS);
(ii) an incoherent, elastic part called resonant hot luminescence, involving inelastic scattering events such as phonon scattering;
(iii) partially or completely thermalized contributions called photoluminescence (PL).

These emissions yield information on the energy level scheme and nature of these levels, as well as on their dynamics. This is well demonstrated in 2D semiconductor quantum wells (QWs): early work on RRS demonstrated exciton localization effects and the existence of a mobility edge [28], while more recent studies dealt with the dynamics of RRS [29,30] and the speckle spectroscopy of disorder [31]. Rayleigh

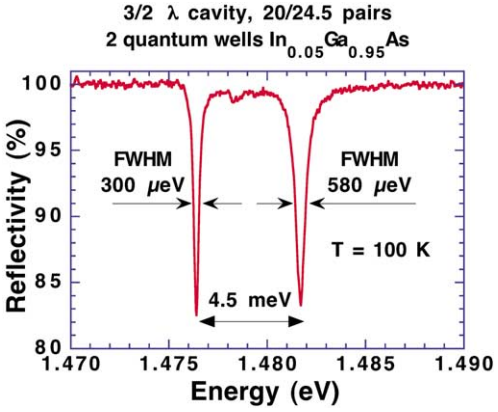

Figure 7. Reflectivity spectrum of a high quality sample, note the 100 K temperature and the extremely narrow linewidths.

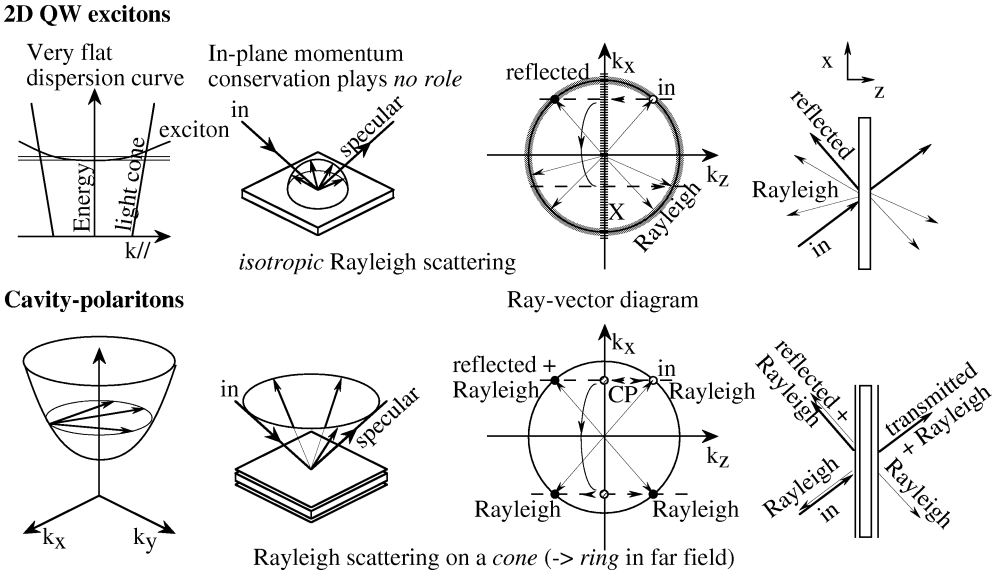

Figure 8. Rayleigh scattering in a bidimensional system: QW exciton vs. cavity-polariton.

scattering of CPs under resonant excitation exhibits remarkable features that impact on light scattering [32].

Let us first consider what happens for *non-resonant* 3D disordered systems in microcavities (the disorder is considered small enough for a cavity mode to develop). In a first approximation, the scattered far-field light is distributed on the Fabry–Pérot cones. Now consider resonantly excited excitons in 2D quantum wells, one deals with a quasi-two dimensional electronic system, in which ideally elastically-scattered excitons lie on a constant energy ring in k-space. However, multiple scattering leads to a randomization of the scattered photon wavevector, with energy being conserved only between initial and final photon states (Fig. 8). This occurs because of the low exciton dispersion on the scale of the photon wavevector. Therefore the RRS intensity is isotropic and does not reflect the bidimensionality of the excitons [30,33–35]. Investigating RRS of a quantum well in a microcavity in the weak-coupling condition, one mainly expects a cavity filtering of the scattered light and therefore a featureless ring of scattered light.

In contrast a microcavity in the strong coupling regime is a near ideal 2D photonic system because of the significant curvature of the CP dispersion curve (Fig. 8). It is therefore expected, and indeed observed that scattering events occur on the quasielastic ring of resonantly excited states.

Fig. 9 shows the far-field image of the microcavity emission and scattered light as a function of angle. The excitation laser spot is in resonance with the lower polariton branch. In this image, a narrow ring of resonantly scattered light can be seen showing some structure along the ring. The exciting beam covers a finite range of incidence angles larger than the cavity-polariton angular width. A neutral density filter has been used to reduce the intensity of the reflected spot in Fig. 1a. A dark arc in the reflected beam can be seen. It coincides with the ring of RRS, and represents the polariton as it would be seen in reflectivity. Careful investigations show that:

(i) The scattered ring is only observed when exciting resonantly the lower polariton branch and for all accessible negative and positive detunings up to $\delta = +2.5$ meV.
(ii) At negative detunings, it conserves the linear polarization of the incident photon.
(iii) The intensity variations along the ring resemble speckle features. They are very sensitive to any variation in position, angle or wavelength of the laser.
(iv) The emission is spectrally identical to the laser.

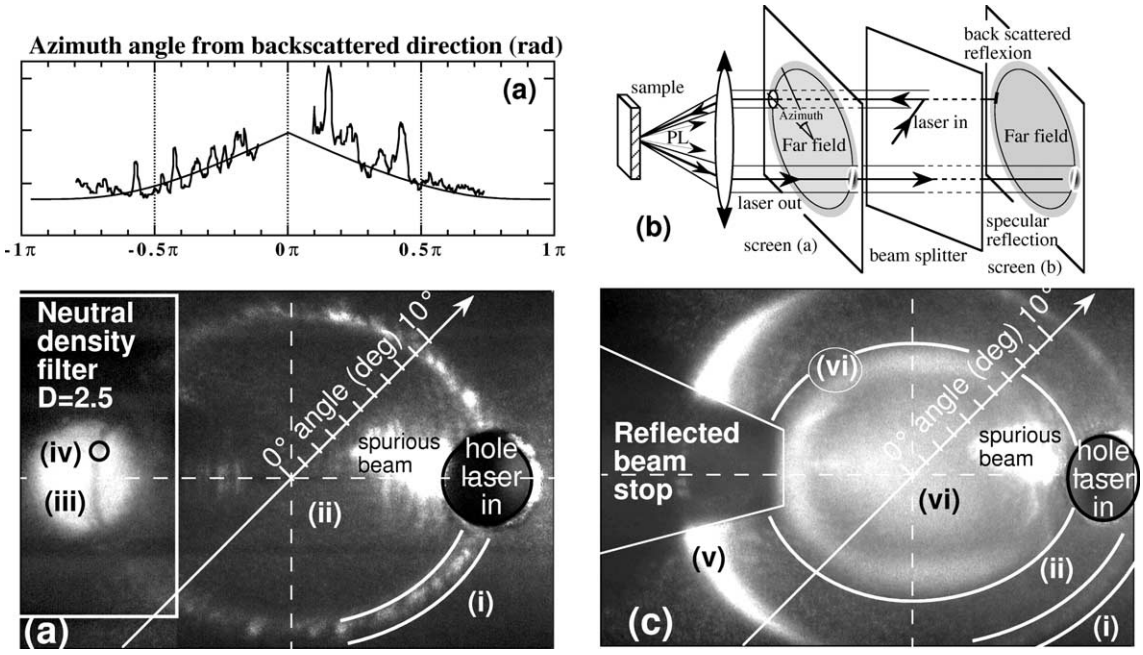

Figure 9. (a) Far field image observed resonant excitation of the lower cavity-polariton branch. Note the elastic Rayleigh arc of circle, its speckle, the attenuated specularly reflected spot, with the absorption beam appearing as a dark arc against an undiminished, non-resonant, reflected beam. (b) Far field emission pattern set-up, screen (a) is used in most measurements, screen (b) is used for backscattering measurements (from R. Houdré et al., Phys. Rev. B 61 (2000) R13333). (c) Far field image in the non-linear regime, above threshold: (i) elastic Rayleigh circle; (ii) photoluminescence from the lower cavity-polariton branch; (v) resonant photoluminescence; (vi) non-linear structure (from R. Houdré et al., Phys. Rev. Lett. 85 (2000) 2793).

(v) The intensity of the ring is strongly temperature dependent. At higher temperatures (20K) the intensity vanishes and the ring becomes a featureless ring of *unpolarized* light.

(vi) Due to the limited dynamic range of the camera, other effects are not visible in the figure. Not observable in the figure because of the weaker intensity, there is PL inside the circle. The PL is non-resonant with the laser, shows the same linewidth as the lower polariton branch, changes wavelength as a function of observation angle and follows the cavity-polariton dispersion curve.

A remarkable feature observed in Fig. 9a is that the reflected intensity is stronger in the backscattered direction showing that additional effects do occur. As seen in Fig. 9a the line shape shows an enhancement of a factor 2 in the backscattered direction with respect of the forward direction, exactly as is expected from CBS. However the angular linewidth of CBS typically reported is in the range of a few mrad (both for 3D and 2D systems). In our observation the angular linewidth is around 90°, leading to a λ_{dB}/l^* value close to 0.2 where λ_{dB} is the de Broglie wavelength of the polariton. It is significantly below the Ioffe–Regel limit $\lambda_{dB} \approx l^*$ for optical Anderson strong localization and is a regime never observed up to now, where lineshape modification of the CBS is expected. Quantitative analysis of the present CBS phenomena is clearly required before making such strong claim and has not been achieved yet as it requires a new formulation of CBS in strongly coupled systems. Moreover, experimental phenomenology is even more complex due to disorder anisotropy effects along $[0 \pm 1 \pm 1]$ crystallographic orientation that are superimposed to a CBS-like lineshape [32].

5. Non-linear regime

In the high density regime CP will exhibit non-linear interaction, for which remains the question as to whether the quasiparticles, being composite Bosons, will behave as Fermions or Bosons on the length scale where non-linear effects manifest. This typically occurs for densities for which the average distance between particles is comparable to the thermal de Broglie wavelength. For QW excitons it is well known that on this scale (≈ 50 nm) exciton behave like Fermions.

The large elastic mean-free path and Broglie wavelength implied by their dispersion has led many to search and claim quantum effects [36–42]. Early non-linear experiments on CP showed a simple linewidth broadening [43] and bleaching of the oscillator strength [44] due to phase space filling and screening. However some non-linear phenomena, in particular, the laser-like non-linear emission observed under both non-resonant and resonant excitation has been the subject of considerable debate. The main mechanisms used to explain such non-linear emission in this system have been the Boser effect [36], and more recently boson assisted stimulation [42], as well as BEC and bi-exciton effects. The Boser effect is the stimulated scattering of bosons into their ground state when the ground-state *occupancy* is greater than unity. For CP the scattering could be mediated by phonons (Boser) or by the CP themselves. Part of the problem is that some previous experiments dwelt on the energy spectrum of the emission, neglecting the dispersion, which is fundamental to the nature of CP, other experiments neglect spatial effects. A complete view is necessary to distinguish between competing theories [45].

Experimental set up and sample are identical to the Rayleigh scattering experiment. On increasing the excitation power, a sudden transition occurs and an intense emission occurs as either a disk, a ring or a more complex pattern (depending on conditions), (region (vi) in Fig. 9c) inside the elastic Rayleigh ring and a crescent shaped resonant photoluminescence becomes clearly visible (region (v)). Performing angular resolved photoluminescence measurements, three components are found in the emitted spectra, of varying amplitude for different emission angles: a Rayleigh component at the exciting energy and centered on the Rayleigh cone, a CP luminescence line the energy of which shifts with angle according to the CP dispersion curve, a strong non-linear emission line which is *dispersionless*, at an energy slightly above the bottom of the CP dispersion curve. This shift rules out an interpretation of the new emission line as a Boser-type effect as it would be unshifted compared to the bottom of the CP band.

Key phenomena can be observed under various experimental conditions and are described in the following summary:

(i) At threshold, depending on the detuning, either an angular point or an actual discontinuity can be observed in the light in–light out curves.

(ii) Around -1 meV detuning, the threshold can reach values as low 17 mW peak incident power, corresponding to an estimated absorbed photon density of $7 \cdot 10^{19}$ cm$^{-2}\cdot$s^{-1}. It is difficult to translate this number into a steady-state population as both lifetime and excited volume depend on excitation intensity via changes in relative populations of CP states with widely different lifetimes, resonance energy shift and spatial pattern formation.

(iii) The non-linear emission energy, angular spread, even emission pattern depend on the excitation conditions. For a given cavity detuning, the non-linear emission *follows* the excitation variation, both in energy (i.e. non-linear emission energy vs. pump energy) and angular extension (i.e. non-linear emission angular spread vs. incident pump angle), although in a non-trivial manner.

(iv) For pump power densities accessible in our experiment, this non-linear behavior is only observed while exciting the lower polariton branch.

(v) From a spatially filtered image, one observes that the strong non-linear emission originates from a region that is no greater than half of the excitation spot (measurement limited by our spatial resolution at the large numerical aperture of the experiment).

(vi) No clear differences are found between linear and circular polarization excitation. This latter result rules out a priori non-linear mechanisms based on biexcitonic effects as it can be assumed that under resonant excitation little spin depolarization occurs, and therefore circular polarization should inhibit biexciton formation as the total biexciton angular momentum must be 0.

It is well known that by pumping a strongly coupled microcavity intensely the system evolves toward the weak coupling regime [44]. Therefore it was important to check whether the cavity was still under strong coupling conditions when reaching threshold. While the persistence of the Rayleigh scattering of the polariton state and observation of a cavity-polariton photoluminescence line would imply that strong coupling was not bleached, it was shown that the experimental features are far more complex [45]. Under high excitation, the polariton absorption observed in the reflected beam is bleached at the center of the excitation spot, while absorption continues to occur in the outer part of the spot. The observation of this inhomogeneous situation greatly helps to solve the puzzle of the many apparently incompatible observed facts, the main one being the coexistence of 'well-behaved' CP photoluminescence with a new emission line incompatible with a CP description: they are due to the coexistence of regions in strong coupling (periphery of excited spot) and regions (center of excited spot) where the resonance energy is spatially shifted, by either carrier renormalization, bleaching or by homogeneous broadening.

Below threshold radiative CP states are directly excited through the resonant excitation. The energy is then redistributed in energy, direction, and eventually space, through inelastic processes (relaxation) or elastic processes (Rayleigh scattering). Neither the thermalized PL nor the elastic ring change in intensity at threshold. Therefore there must be another channel not visible in our experiment into which the pump energy is scattered below threshold. Such channels could be leaky and guided modes that remain trapped inside the GaAs material.

Regarding the non-linear mechanism, CP–CP scattering, which conserves both energy and momentum, can be viewed as parametric amplification (or non-degenerate four wave mixing) where 2 CPs scatter simultaneously from $k = k'$ to $k = 0$ and $k = 2 \cdot k'$. Such phenomena have been recently observed by Savvidis et al. [42], in pump-probe experiments, where the CPs were excited resonantly at $k = k'$ and $k = 0$, with resulting emission at $k = 2k'$. Their results and ours triggered a novel theoretical treatment [46] based on a phase-matched four wave mixing or parametric amplification. In our experiments, the thermal PL acts as an idler (probe) that seeds the parametric process. After a certain pump intensity there is sufficient power to provide gain at $k = 0$. Many of the features observed in our experiments such as the blue shift of the non-linear emission with respect to the cavity mode by a quantity of the order of the CP homogeneous linewidth are also predicted in this model [46] as well as off branch polaritons multiple scattering [47]. In addition quantum noise measurement shows a phase dependence of the amplification that is typical of coherent multiwave mixing process [48].

6. Conclusion

Planar semiconductor microcavities in the weak and strong coupling regimes have been a rich playground for the semiconductor physicist. While the original inspiration came from the atomic physics, the novel phenomena have come from the interplay of the dimensionality of the electronic and optical excitations that can be engineered in solid-state systems. Most of the work has concentrated on 2D photons interacting with 0D, 1D, 2D and 3D electronic transitions. It will be therefore interesting to move towards higher-dimensional cavities with equivalent characteristics (finesse, Q-factor, etc.) to the best planar structures. Etching planar cavities into pillars is already a standard way to make 3D cavities. The advent of photonic band gap materials leaves room for other geometries and perhaps even better cavities.

Acknowledgements. This work was supported by EPFL (Switzerland), the EEC Esprit programs SMILES and SMILED and the Swiss national priority program for optics.

References

[1] K.H. Drexhage, in: E. Wolf (Ed.), Progress in Optics, North-Holland, 1974.
[2] P. Wittke, RCA Rev. 36 (1975) 655.
[3] R.E. Kunz, W. Lukosz, Phys. Rev. B 21 (1980) 4814.
[4] D. Kleppner, Phys. Rev. Lett. 47 (1981) 233.
[5] S. Haroche, in: G. Grynberg, R. Stora (Eds.), New Trends in Atomic Physics, North-Holland, Amsterdam, 1983.
[6] P.R. Berman (Ed.), Cavity Quantum Electrodynamics, Academic Press, Boston, 1995.
[7] H. Yokoyama, K. Ujihara (Eds.), Spontaneous Emission and Laser Oscillation in Microcavities, CRC Press, Boca Raton, 1995.
[8] C. Weisbuch, E. Burstein (Eds.), Confined Electrons and Photons, Plenum, Boston, 1995.
[9] E.M. Purcell, Phys. Rev. 69 (1946) 681.
[10] R.J. Thompson, G. Rempe, H.J. Kimble, Phys. Rev. Lett. 68 (1992) 1132.
[11] J.J. Hopfield, in: R.J. Glauber (Ed.), Quantum Optics, Academic Press, New York, 1969.
[12] R.S. Knox, Theory of Excitons, Academic Press, New York, 1963.
[13] C. Weisbuch, M. Nishioka, A. Ishikawa, Y. Arakawa, Phys. Rev. Lett. 69 (1992) 3314.
[14] R. Houdré, R.P. Stanley, U. Oesterle, M. Ilegems, C. Weisbuch, Phys. Rev. B 49 (1994) 16761.
[15] Y. Zhu, D.J. Gauthier, S.E. Morin, Q. Wu, H.J. Carmichael, T.W. Mossberg, Phys. Rev. Lett. 64 (1990) 2499.
[16] J.J. Sanchez-Mondragon, N.B. Narozhny, J.H. Eberly, Phys. Rev. Lett. 51 (1983) 550.
[17] V. Savona, L.C. Andreani, P. Schwendimann, A. Quattropani, Solid State Commun. 93 (1995) 733.
[18] S. Jorda, Phys. Rev. B 50 (1994) 18690.
[19] D.S. Citrin, in: C. Weisbuch, E. Burstein (Eds.), Confined Electrons and Photons, Plenum, Boston, 1994.
[20] R. Houdré, C. Weisbuch, R.P. Stanley, U. Oesterle, P. Pellandini, M. Ilegems, Phys. Rev. Lett. 73 (1994) 2043.
[21] R.P. Stanley, R. Houdré, C. Weisbuch, U. Oesterle, M. Ilegems, Phys. Rev. B 53 (1996) 10995.
[22] V. Savona, C. Weisbuch, Phys. Rev. B 54 (1996) 10835.
[23] D.M. Whittaker, P. Kinsler, T.A. Fisher, M.S. Skolnick, A. Armitage, A.M. Afshar, M.D. Sturge, J.S. Roberts, Phys. Rev. Lett. 77 (1996) 4792.
[24] D.M. Whittaker, Phys. Rev. Lett. 80 (1998) 4791.
[25] V. Savona, C. Piermarocchi, A. Quattropani, F. Tassone, P. Schwendimann, Phys. Rev. Lett. 78 (1997) 4470.
[26] R. Houdré, R.P. Stanley, M. Ilegems, Phys. Rev. A 53 (1996) 2711.
[27] C. Ell, J. Prineas, T.R. Nelson Jr., S. Park, H.M. Gibbs, G. Khitrova, S.W. Koch, R. Houdré, Phys. Rev. Lett. 80 (1998) 4795.
[28] J. Hegarty, M.D. Sturge, J. Opt. Soc. Am. B 2 (1985) 1143.
[29] S. Haacke, R.A. Taylor, R. Zimmermann, J.I. Bar, B. Deveaud, Phys. Rev. Lett. 78 (1997) 2228.
[30] G. Hayes, S. Haacke, M. Kauer, R.P. Stanley, R. Houdré, U. Oesterle, B. Deveaud, Phys. Rev. B 58 (1998) R10175.
[31] W. Langbein, J.M. Hvam, R. Zimmermann, Phys. Rev. Lett. 82 (1999) 1040.
[32] R. Houdré, C. Weisbuch, R.P. Stanley, U. Oesterle, M. Ilegems, Phys. Rev. B 61 (2000) R13333.
[33] J. Hegarty, M.D. Sturge, C. Weisbuch, A.C. Gossard, W. Wiegmann, Phys. Rev. Lett. 49 (1982) 930.
[34] V. Savona, R. Zimmermann, Phys. Rev. B 60 (1999) 4928.
[35] S. Haacke, G. Hayes, R.A. Taylor, B. Deveaud, R. Zimmermann, J.I. Bar, Phys. Status Solidi B 204 (1997) 35.
[36] A. Imamoglu, R.J. Ram, Phys. Lett. A 214 (1996) 193.
[37] S. Pau, G. Björk, J. Jacobson, H. Cao, Y. Yamamoto, Phys. Rev. B 51 (1995) 7090.
[38] M. Kira, F. Jahnke, S.W. Koch, J.D. Berger, D.V. Wick, T.R. Nelson, G. Khitrova, H.M. Gibbs, Phys. Rev. Lett. 79 (1997) 5170.
[39] Si Dang Le, D. Heger, R. André, F. Boeuf, R. Romestain, Phys. Rev. Lett. 81 (1998) 3920.
[40] P. Senellart, J. Bloch, Phys. Rev. Lett. 82 (1999) 1233.
[41] F. Tassone, Y. Yamamoto, Phys. Rev. B 59 (1999) 10830.
[42] P.G. Savvidis, J.J. Baumberg, R.M. Stevenson, M.S. Skolnick, D.M. Whittaker, J.S. Roberts, Phys. Rev. Lett. 84 (2000) 1547.
[43] F. Jahnke, M. Kira, S.W. Koch, G. Khitrova, E.K. Lindmark, T.R. Nelson, D.V. Wick, J.D. Berger, O. Lyngnes, H.M. Gibbs, K. Tai, Phys. Rev. Lett. 77 (1996) 5257.
[44] R. Houdré, J.L. Gibernon, P. Pellandini, R.P. Stanley, U. Oesterle, C. Weisbuch, J.O. Gorman, B. Roycroft, M. Ilegems, Phys. Rev. B 52 (1995) 7810.
[45] R. Houdré, C. Weisbuch, R.P. Stanley, U. Oesterle, M. Ilegems, Phys. Rev. Lett. 85 (2000) 2793.
[46] C. Ciuti, P. Schwendimann, B. Deveaud, A. Quattropani, Phys. Rev. B (2000), in press.
[47] P.G. Savvidis, C. Ciuti, J.J. Baumberg, D.M. Whittaker, M.S. Skolnick, J.S. Roberts, Phys. Rev. Lett. 64 (2001) 075311.
[48] G. Messin, J.P. Karr, A. Baas, G. Khitrova, R. Houdré, R.P. Stanley, U. Oesterle, E. Giacobino, Phys. Rev. Lett. 8712 (2001) 7403.